IJAREEIE

e-ISSN: 2278-8875
p-ISSN: 2320-3765

International Journal of Advanced Research

in Electrical, Electronics and Instrumentation Engineering

Volume 10, Issue 4, April 2021

INTERNATIONAL STANDARD SERIAL NUMBER INDIA

Impact Factor: 7.122

| e-ISSN: 2278 – 8875, p-ISSN: 2320 – 3765| www.ijareeie.com | Impact Factor: 7.122|

|| Volume 10, Issue 4, April 2021 ||

DOI:10.15662/IJAREEIE.2021.1004028

Thermal Wave Imaging for Detection and Evaluation of Bone Density

Mrs.R.PRATHIPA[1] , M.Arun[2], Chidambara Eswari.M[3], Archana.J[4] , Abirami.A[5]

Associate professor, Dept. of ECE, Panimalar Institute of Technology, Chennai, Tamilnadu, India[1]

Assistant professor, Dept. of ECE, Panimalar Institute of Technology, Chennai, Tamilnadu, India[2]

UG Student, Dept. of ECE, Panimalar Institute of Technology, Chennai,Tamilnadu, India[3,4,5]

ABSTRACT: Bone Density is defined as the amount of bone mineral present in the bone tissue. Age, sex, illness, genetics, and lifestyle are all factors that influence bone density[1]. X-rays are used to determine how many grams of calcium and other bone minerals are packed into a segment of bone in a bone density test. The neck, shoulder, and sometimes the forearm are the bones that are most sorely tested. The sum of bone mineral (calcium hydroxyapatite Ca10 (PO4)6 (OH)2) per unit volume of bone tissue is used to calculate bone mineral density(BMD)[2]. Medical conditions such as diabetes, peak bone mass, and postmenopausal estrogenic deficiency influence bone mineral density. Early testing or estimation of bone density is important as a person's age increases in order to retain good bone strength, so this system aims to assess the capabilities of one of the most commonly used thermal imaging techniques to characterise the density of human bone. The image is pre-processed with a gaussian filter in this method, which blurs the image or reduces noise. The system then proves that active infrared thermography, also known as thermal wave imaging, is a promising non-contact, non-invasive, remote, patient-friendly, and safe imaging modality for measuring and evaluating various biomaterials. This system can be used to evaluate bone diseases caused by calcium deficiency by measuring or predicting bone brittleness using thermal imaging and RGB imaging, as well as by displaying variations in our histogram gradients.

KEYWORDS: Bone Density, Thermal wave imaging, Gaussian filter, Image Processing, Pixel Segmentation.

I.INTRODUCTION

Bone density is a metric that indicates how thick and strong a person's bones are. Low bone density (also known as osteopenia) is defined as a bone density that is lower than the standard peak density but not low enough to be diagnosed as osteoporosis[1,3]. Bone diseases may be caused by a variety of factors. Bone density is affected not only by age, but also by drugs used to treat breast cancer, hypertension, asthma, Crohn's disease, and Addison's disease[5]. Bone thinning may also be caused by illnesses like hyperthyroidism, hypopituitarism, and eating disorders. The main bone diseases caused by loss of bone density are bone cancer, bone infections, Osteogenesis Imperfecta, Osteonecrosis, Paget's Disease of Bone, and Rickets[8]. As a result, early detection of bone mineral density would aid in the diagnosis of such diseases.

Non-invasive, remote, and non-ionizing radiation imaging techniques for characterization of biomedical materials are critical for disease early detection[12]. Infrared thermography (IRT) has grown in popularity as a result of its remote, secure, and wide-area inspection capabilities. It has a wide variety of uses, ranging from industrial condition monitoring to medical imaging.

For detecting bone mineral density (BMD), we use Image Processing and thermal wave imaging techniques in our method . A thermal camera is used to record the thermal RGB images of bones. The noise is extracted using a Gaussian filter to create smoothed thermal RGB images. As a consequence, the Gaussian blur (also known as Gaussian smoothing) is the result of blurring an image with a Gaussian function in image processing (named after mathematician and scientist Carl Friedrich Gauss). It's a common effect in graphics software for reducing image noise and reducing detail. To reduce the colour complexity, the images are now transformed to grayscale images. Using the Fourier transform, the padding is set to '0' for equivalent matrix size, then the high-pass filter is applied, and finally the bone density is measured. Digital image segmentation is the method of subdividing a digital image into its constituent objects, and it is one of the most important tasks of digital image processing. Hence, image segmentation is a low-level vision task that can be used in a variety of applications, including object recognition, medical imaging, and document processing. As a result, we used Particle Swarm Optimization, which is a very effective computational tool for optimising a problem by iteratively trying to develop a candidate solution in terms of a given quality metric.

| e-ISSN: 2278 – 8875, p-ISSN: 2320 – 3765| www.ijareeie.com | Impact Factor: 7.122|

|| Volume 10, Issue 4, April 2021 ||

DOI:10.15662/IJAREEIE.2021.1004028

II.METHODOLOGY

A. Gaussian Filter Application

Various types of noise may appear in digital images. Noise is caused by errors in the image acquisition process, which cause pixel values to differ from the true intensities of the real scene. The picture is blurred using the Gaussian Filter. Its aim is to minimise noise and image details. Gaussian filters are typically isotropic, meaning that their standard deviation is the same in both dimensions. By specifying a scalar value for sigma, an isotropic Gaussian filter can be applied to an image. The Gaussian kernel can have different standard deviations along row and column dimensions with imgaussfilt. They are referred by the name Axis-aligned anisotropic Gaussian filters. When using anisotropic filters, we specify a 2-element vector for sigma. The corresponding input pixel will be about the value of the output pixel to the average of the pixel values in the neighbourhood. The value of an output pixel is calculated by the median of the neighbourhood pixels, rather than the mean, with our median filtering. The median is less sensitive to extreme values (called outliers) than the mean. As a result, median filtering is better at removing outliers of our image without reducing image sharpness.

B.Pixel Segmentation

Particle swarm optimization (PSO) is an optimization algorithm that uses a population-based approach. PSO's algorithm starts with a group of random particles and then updates generations to look for optima. Each particle is flown through the search space, with its location changed based on its distance from its personal best position as well as the distance from the swarm's best particle. Each particle's efficiency, or how close it is to the global optimum, is calculated using a fitness function that is dependent on the optimization problem.

Each particle, i, travels through a n–dimensional search space, R n, and keeps track of the following information:

- Xi, ith particle's current position (x - vector),
- pi, ith particle's personal best position (p - vector),
- vi, ith particle's current velocity (v - vector).

The particle's personal best position, i, is the best position that the particle has visited so far.

The representation step, or finding a suitable mapping between a problem and PSO particles, is one of the most important aspects of designing a successful PSO algorithm. K thresholds are represented by a single particle. That is, each vector xi is constructed as xi = (t_i,1,..., $t_{i,j}$,..., $t_{i,k}$), where $t_{i,j}$ denotes the i^{th} particle's j^{th} threshold value. As a result, a swarm represents a number of segmented images after each particle has been thresholder. Hence, the application of this algorithm to the image segmentation problem can be sequenced in the following manner:

Step 1: Read the input image that has to be segmented.

Step 2: Apply the PSO method to that image with a specific threshold level.

Step 3: Step 3: Update the fitness of each particle in the population, in the search space and Particle's best in the search space is updated, and the particle is moved into the population.

Step 4: For each particle, if the swarm improves, reward the swarm by spawning the particle, thus extending the swarm/particle life

Step 5: For each particle, if the swarm's efficiency isn't improving, punish the swarm: Delete the swarm/particle: or shorten the life of the swarm.

C. STRUCTURAL SIMILARITY INDEX

SSIM is also measured in the Imatest Image processing module, which has several features not present in the SSIM module. For example,It may apply common image degradations (noise, blur, flare, and so on) before applying signal processing techniques that are widely used to improve images (tone mapping, unsharp mask, bilateral filtering, etc.).

D. GLCM

Image analysis techniques include the Gray Level Co-occurrence Matrix (GLCM) and associated texture feature calculations. The GLCM is a tabulation of how often different combinations of gray - level co-occur in an image or image segment given an image composed of pixels each with an intensity (a specific grey level). The contents of the GLCM are used in texture feature calculations to provide a measure of the difference in intensity (a.k.a. image texture) at the pixel of interest.

E. HISTOGRAM GRADIENT:

A histogram is a visual representation of statistical data that shows the frequency of data items at different intervals. Plotting histograms is a function in MATLAB that allows the user to generate a bar graph for any vector or matrix and group the data into bins using an automatic binning algorithm. The histogram values in range of 5/6 is considered to be

| e-ISSN: 2278 – 8875, p-ISSN: 2320 – 3765| www.ijareeie.com | Impact Factor: 7.122|

|| Volume 10, Issue 4, April 2021 ||

DOI:10.15662/IJAREEIE.2021.1004028

defective and this is also exhibited by the use of histogram colour gradient with varying pixel quality. The area represents the frequency of occurrence of the data in each bin, not the height. It allows for histogram presentation's customization.

Approach:

- Read the source image file into image matrix.
- Convert it to grayscale if it is an RGB image.
- Iterate over image matrix and count the frequency of every possible value of intensity.
- Plot the counted frequency.

.

III. RESULT

The below picture shows the output of our final project

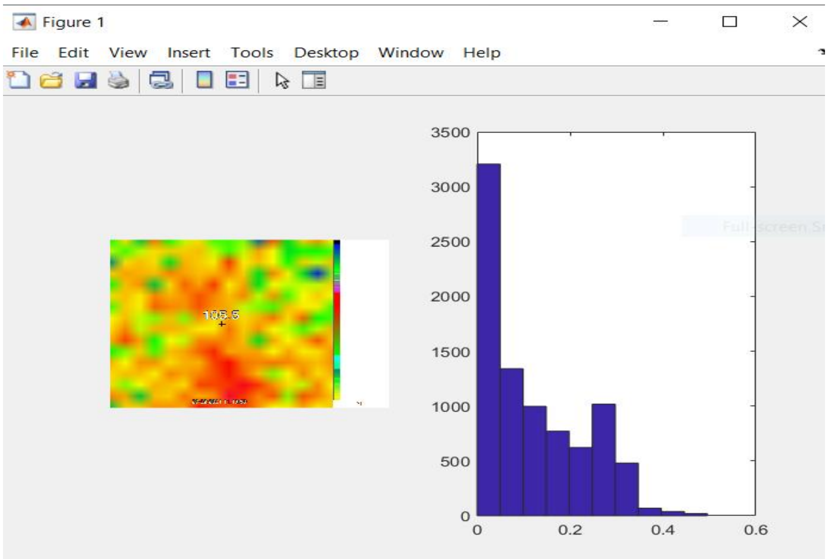

Figure 1

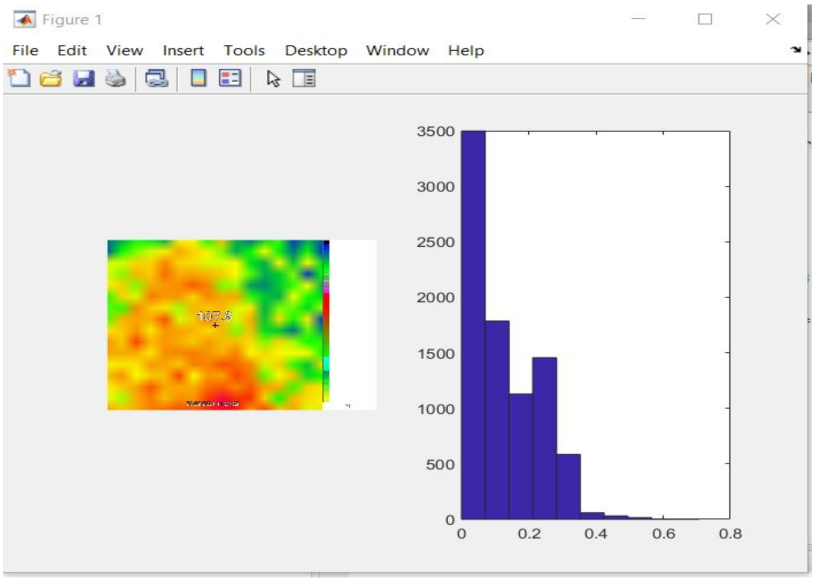

Figure 2

| e-ISSN: 2278 – 8875, p-ISSN: 2320 – 3765| www.ijareeie.com | Impact Factor: 7.122|

|| Volume 10, Issue 4, April 2021 ||

DOI:10.15662/IJAREEIE.2021.1004028

IV.CONCLUSION

The proposed device emphasises the capability of thermal wave imaging in detecting density variations in bone, allowing for the identification of the severity of bone diseases based on density variations. To improve the estimation of human bone density, various image processing techniques such as Histogram Gradient and pixel segmentation using particle swarm optimization are used. Thermal wave imaging is clearly used to detect human bone density with the aim of developing a technology for the early, healthy, and remote diagnosis of bone diseases with increased sensitivity and resolution.

REFERENCES

[1]G. Dua and R. Mulaveesala, "Infrared thermography for detection and evaluation of bone density variations by non-stationary thermal wave imaging," Biomedical Physics & Engineering Express, vol. 3, no. 1, p. 017006, 2017.
[2] V. Arora., and R. Mulaveesala, "Pulse compression with Gaussian weighted chirp modulated excitation for infrared thermal wave imaging," Progress in Electromagnetics Research Letters, 44, pp. 133-
137, 2014.
[3] R. Mulaveesala and S. Tuli, "Digitized frequency modulated thermal wave imaging for nondestructive testing," Materials Evaluation, vol. 63, no. 10, 2005.
[4] X.P.V. Maldague, "Theory and Practice of Infrared Thermography for Nondestructive Testing," Wiley, New York, 2001.
[5] F. B, et al., "Evaluation of bone density using cutting resistance measurements and microradiography: an in vitro study in pig ribs," Clin Oral Implants Res, vol. 6, pp. 164-71, 1995.
[6] A. L. Adams et al., "Osteoporosis and hip fracture risk from routine computed tomography scans: the fracture, osteoporosis, and CT utilization study (FOCUS)," Journal of Bone and Mineral Research, vol. 33, no. 7, pp. 1291-1301, 2018.
[7] V. Arora, J. A. Siddiqui, R. Mulaveesala, and A. Muniyappa, "Pulse compression approach to nonstationary infrared thermal wave imaging for nondestructive testing of carbon fiber reinforced polymers," IEEE Sensors Journal, vol. 15, no. 2, pp. 663-664, 2014.
[8] S. R. Cummings and L. J. Melton, "Epidemiology and outcomes of osteoporotic fractures", *Lancet*, vol. 359, no. 9319, pp. 1761-1767, 2002.
[9] R. Mazess, B. Collick, J. Trempe, H. Barden and J. Hanson, "Performance evaluation of a dual-energy X-ray bone densitometer", *Calcified Tissue Int.*, vol. 44, no. 3, pp. 228-232, 2018.
[10] J. E. Mulder, D. Michaeli, E. R. Flaster and E. Siris, "Comparison of bone mineral density of the phalanges lumbar spine hip and forearm for assessment of osteoporosis in postmenopausal women", *J. Clin. Densitometry*, vol. 3, no. 4, pp. 373-381, 2000.
[11] A. Nazarian, D. Von Stechow, D. Zurakowski, R. Müller and B. D. Snyder, "Bone volume fraction explains the variation in strength and stiffness of cancellous bone affected by metastatic cancer and osteoporosis", *Calcified Tissue Int.*, vol. 83, no. 6, pp. 368-379, 2016.
[12]Wei Wang; Gangqiang Hu; Bo Yuan; Shandong Ye; Chao Chen; Yayun Cui; Xi Zhang; Liting Qian, "Prior-Knowledge-Driven Local Causal Structure Learning and Its Application on Causal Discovery Between Type 2 Diabetes and Bone Mineral Density", IEEE Access (Volume: 8), 18 May 2020.
[13] Mikael J. Turunen; Juha Töyräs; Harri T Kokkonen; Jukka S. Jurvelin, "Quantitative Evaluation of Knee Subchondral Bone Mineral Density Using Cone Beam Computed Tomography", IEEE Transactions on Medical Imaging (Volume: 34, Issue: 10, Oct. 2017).
[14] D. Dore, S. Quinn, C. Ding, T. Winzenberg and G. Jones, "Correlates of subchondral BMD: A cross-sectional study", *J. Bone Miner. Res.*, vol. 24, no. 12, pp. 2007-2015, Dec. 2019.
[15]Jose Sulla-Torres; Christian Incalla Nina; Margoth Rivera Portugal; Marco Cossio-Bolaños; Rossana Gómez Campos, "Comparison Of Classification Algorithms For The Detection Of Bone Weakness In Students Using Anthropometric Data", International Conference on Inclusive Technologies and Education (CONTIE), 30 January 2020

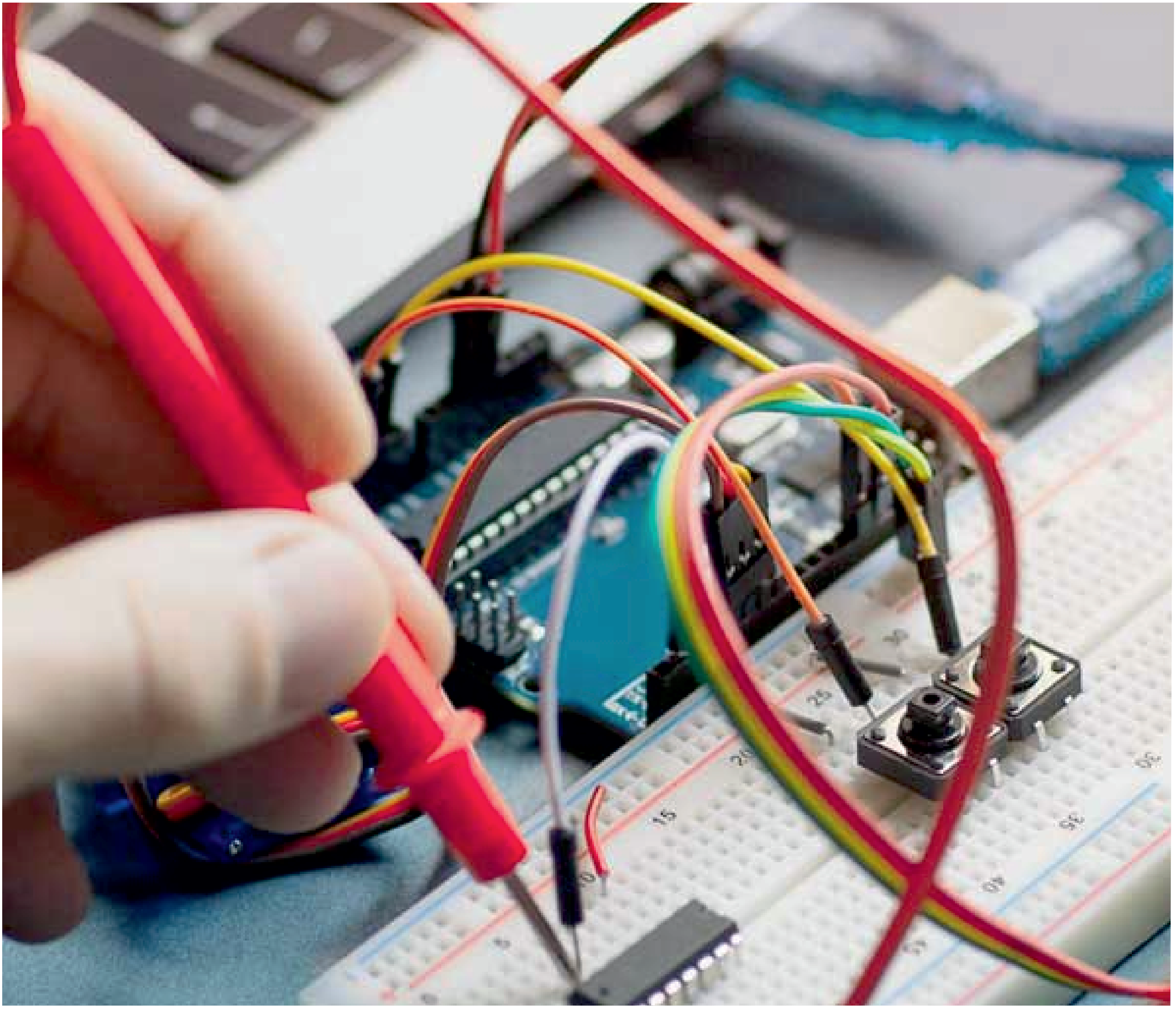

INNO SPACE
SJIF Scientific Journal Impact Factor

Impact Factor:
7.122

INTERNATIONAL STANDARD SERIAL NUMBER INDIA

निस्केयर
NISCAIR

International Journal of Advanced Research

in Electrical, Electronics and Instrumentation Engineering

9940 572 462 6381 907 438 ijareeie@gmail.com

www.ijareeie.com

Scan to save the contact details